Keck NGAO sky coverage modeling

Richard M. Clare

February 6 2007

KAON 470

1. Introduction

This report details the sky coverage simulations carried out for the Keck Next Generation Adaptive Optics (NGAO) system. This work was carried out to meet the objectives stated in WBS Element Number: 3.1.2.2.10 - *Number and Type of Low Order WFS TS*. As well as investigating the number of Natural Guide Star (NGS) Shack-Hartmann wavefront sensors (WFS), this report considers the number of modes to measure with the NGS WFS, the spectral band for the NGS WFS, the size of the NGS patrol field, and the amount of partial correction of the NGS. These sky coverage trade studies are completed for a selection of the science cases identified in Ref. 1. This report does not consider the type of low order wavefront sensor; Shack-Hartmann WFS(s) are assumed throughout, and a separate study will consider Shack-Hartmann vs pyramid WFSs.

The sky coverage simulations presented here are calculated with the Sky Coverage Simulator developed for TMT and documented in Ref.s 2, 3. This code is a covariance based code, which allows fast simulation of large numbers of NGS constellations. The NGS constellations are generated using star statistics: for J,H, and K bands the Spagna[4] model is used, and for V band the Bahcall-Soneira model[5] model is used. The essence of this method is to transform the turbulence phase screens at each altitude, which are represented as a Zernike basis sum, to the aperture using geometric optics. This model accounts for the cone effect for the finite height of the laser guide stars LGSs, as well as the anisoplanatism caused by the GSs being off-axis with respect to the science object. The expected wavefront error is then calculated using a minimum variance estimator from these transformation matrices and the statistical properties of the atmosphere and the noise.

The tip-tilt (TT) errors that are calculated are the sum of three terms: the servo lag, measurement noise and tilt anisoplanatism. The tilt anisoplanatism term includes the effect of the pairs of quadratic "null modes" that

are induced in multiple LGS AO systems. The sampling frequency is optimized for each NGS constellation to balance the errors due to servo lag and measurement noise.

The sky coverage simulator had a number of features for TMT which have been removed for this Keck NGAO trade study. The wind-shake error and focus error from incorrectly tracking the sodium layer altitude variations have been removed as they are TMT specific. They have not been replaced with any Keck models. The controller transfer function of TMT, which incorporated the woofer-tweeter control, has been replaced with a single integrator control with a gain of 0.5.

The sky coverage simulator was compared with LAOS, the Linear Adaptive Optics Simulator developed by Ellerbroek and Gilles, matching the simulator parameters as well as possible for four different NGS constellations. LAOS is a full wave optics simulation, whereas the sky coverage simulator is a covariance based code. The codes agreed well in the noiseless case, i.e. the tilt anisoplanatism and servo lag terms agreed well between codes. The agreement was not as good when considering the measurement noise. In particular, for the dim stars case the TT error for LAOS was 480 ± 52 nm compared to 334 nm for the sky coverage simulator. This difference was felt to be due largely because the matched filter algorithm that was used for both (as opposed to standard centroiding as in this report) did not perform well in LAOS for low signal levels.

The results of the sky coverage simulator for NGAO were also compared to the spreadsheets of Rich Dekany in the NGAO proposal.[1] These calculations are based on scaling law techniques to estimate the TT. For the field galaxies science case, the 30th percentile TT presented in the NGAO proposal is 70 nm, and the 30th percentile for the same case calculated with the sky coverage simulator is 76 nm, showing good agreement in this case.

We consider three of the science cases presented in Ref. 1: the field galaxies case, GOODS-N case, and narrow field case. The different science cases have different total high order wavefront errors, different galactic latitudes, and different science field diameters.

In the next section, we describe the simulation parameter set, and discuss the different trade studies performed so far.

Table 1. System and atmospheric parameters.

Parameter	Symbol	Value
Telescope diameter	D	10 m
Read noise	σ_e	10 e^- per pixel readout
Outer scale	L_0	75 m
Pixel subtense (V band)	w	0.5 arc sec
Pixel subtense (J, H or K bands)	w	λ/D rads
Fried's parameter	r_0	0.156 m
r_0 Evaluation wavelength	λ_e	0.5 μm
Height of sodium LGS	H	90 km
DM conjugate altitudes	h_m	0,10 km
Zernike radial order	N	6
End-to-end efficiency of optics	χ	0.4
Sampling frequency range	f_s	10 - 1000 Hz
Background intensity (V band)	z_b	21.9 mags arc sec^{-2}
Background intensity (J band)	z_b	16.3 mags arc sec^{-2}
Background intensity (H band)	z_b	14.4 mags arc sec^{-2}
Background intensity (K band)	z_b	12.9 mags arc sec^{-2}
Intensity of m=0 star (V band)	z	9.71×10^9 photons m^{-2} s^{-1}
Intensity of m=0 star (J band)	z	3.76×10^9 photons m^{-2} s^{-1}
Intensity of m=0 star (H band)	z	3.17×10^9 photons m^{-2} s^{-1}
Intensity of m=0 star (K band)	z	1.30×10^9 photons m^{-2} s^{-1}
Imaging wavelength (V band)	λ	0.5 μm
Imaging wavelength (J band)	λ	1.25 μm
Imaging wavelength (H band)	λ	1.65 μm
Imaging wavelength (K band)	λ	2.2 μm

2. Simulations

The turbulence profile used in these simulations is the Mauna Kea profile described in Ref. 7. This profile has an r_0 of 15.6 cm. The wind profile used here is also a Mauna Kea profile and is listed in Ref. 6. The rest of the constant parameters used in this study are tabulated in Table 1. In all cases, the magnitude limit is 19, and all combinations of NGS below this limit are evaluated in order to choose the best combination. In all the simulations over all the bands, the read noise is assumed to be 10 electrons per pixel per readout. In all the simulations, we assume Shack-Hartmann WFS with quad-cell centroiding.

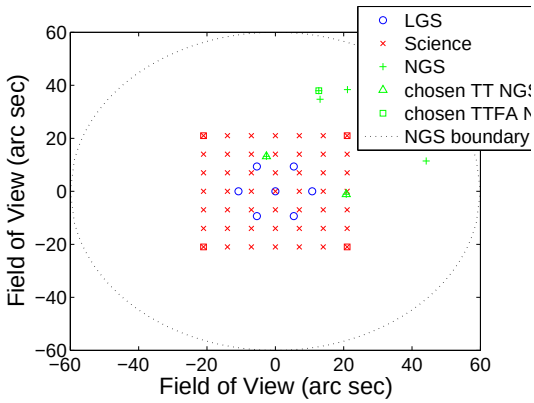

Fig. 1. The field of view for the median case for the field galaxies science field of 42 arc sec square for 2 TT sensors and 1 TTFA sensor.

The LGS asterism chosen is asterism 7a in Ref. 7, which is shown in Fig. 1. This asterism consists of seven LGS: 1 on-axis and the remaining six equally spaced on a ring. The radius of this ring determines the partial correction of the NGSs. We consider three of the five LGS ring radii investigated in Ref. 7: 7.2 arcsec, 21.6 arcsec, and 35.9 arcsec. The middle value of 21.6 arcsec is chosen as the default. The level of partial correction of the NGSs as a function of their position in the field is calculated as follows. The tomography error as a function of radii is taken from Figure 10 (bottom) in Ref. 7. This tomography error is then added to total higher order wavefront error stated in the science case spreadsheets of Ref. 1 (minus the LGS tomography error listed in the spreadsheet so that the tomography error is not counted twice). The total higher order wavefront error is assumed to be constant across the field. This approach leads to the partial correction curves of Fig. 2 for the field galaxies, GOODS-N and narrow field science cases for the three LGS asterism radii of 7.2, 21.6 and 35.9 arcsec. Similar partial correction curves were also obtained in H and K band, by converting the higher order errors into H and K Strehls.

The TT errors discussed in the subsequent sections are reported in nm rms. To convert from nm to mas, the TT error in nm should be divided by 12.1.

2.A. Wavelength band

Four wavelength bands for NGS wavefront sensing are investigated: V, J, H, and K, as well as the combination of J+H, and also J+H+K. In the visible (V band), we assume that we are seeing limited, and in the Near IR (J,H,K), we

assume we are partially corrected. The difference between the three near IR bands is a trade-off between five quantities: spot size, background, zeropoints, abundance of stars of a given magnitude, and amount of partial correction. As the wavelength increases, the spot size increases, the background is larger, the zeropoint (ie number of photo-detection events for a zero magnitude star) decreases, there are more stars of a given brightness, and the partial correction of the NGS improves. So, two of the five quantities dependent on the spectral band (partial correction and abundance of stars) are better at the longer wavelength, and three (spot size, zeropoint, background) are better at the shorter wavelength. In this calculation, the magnitude of the stars in V band is calculated with the Bahcall-Soneira star density model. The magnitudes in J band are calculated with the Spagna model. The magnitudes in H and K are calculated by reddening the J magnitudes with the J-H and J-K magnitude differences for a G0 dwarf, which lies in the middle of the table for these magnitude differences as reported in Bessell and Brett.[8] From simulations for TMT, this calculation is largely insensitive to the class of object as the range of J-H and J-K values is small (the range of J-H is 0.66 and J-K 1.03).

In Table 2, the median, 10th and 90th percentile TT errors are shown for these spectral bands for wavefront sensing. In all cases, we consider a 2 arc min diameter NGS patrol field, the field galaxies science case with a 2 arc sec science field, and an LGS asterism of diameter 21.6 arc sec. We also use 2 TT NGS WFS (i.e. 1x1 lenslets) and 1 tip-tilt-focus-astigmatism (TTFA) sensor (i.e. 2x2 lenslet array). Clearly, using any of the near IR bands is preferable to the visible V band, which is due to the expected partial correction in the near IR. Of the three near IR bands considered separately, J and H give equivalent TT performance, and better than K. Using a combination of J and H significantly improves the TT estimate, but there is little extra improvement in also including the K band.

2.B. Field Diameter

We consider the size of the NGS patrol field. This calculation does not take into account the extra benefit of a bright star off-axis in reducing the level of wind-shake; it only takes into account the fundamental errors of servo lag, measurement noise and tilt anisoplanatism. Also, this calculation did not take into account the optimization of the LGS asterism radius for each NGS constellation - a radius of 21.6 was assumed throughout. The curves

Table 2. Residual TT error for the spectral band(s) for the NGS WFS using 2 TT sensors and 1 TTFA sensor.

WFS option	TT error (nm)		
	10th percentile	median	90th percentile
V band	172	306	1133
J band	47	102	199
H band	46	99	190
K band	65	133	239
J+H bands	36	79	164
J+H+K bands	34	75	158

were generated using the field galaxies science case with a science field of 42 arc sec, not the 2 arc sec of the previous subsection. Consequently, the TT errors reported in this subsection are significantly larger than in the previous subsection, due to the increase in tilt anisoplanatism for the much larger science field.

The median, and 10th and 90th percentile residual TT errors are plotted versus the patrol field diameter in Fig. 3. The curves are flat at over 1100 nm (the open loop error), where the median, or 10th or 90th percentile case corresponds to no stars of magnitude less than 19 in the patrol field. After the patrol field diameter is increased past 100 arc sec, there is little benefit to increasing the field diameter. This is because of the reduction in the partial correction of the stars at this offset, and the extra tilt anisoplanatism induced from selecting a star this far off-axis.

2.C. Number and type of NGS WFSs

We consider the number of NGS WFS and the number of modes to measure with them. The median and 10th and 90 percentile residual TT errors are tabulated in Table 3 for 1 to 5 TT NGS WFS only (ie 1x1 lenslets). In all cases, the standard parameter set is used and with a 2 arc min diameter patrol field, J band sensing, and for the field galaxies case with a 2 arc sec square science FOV. There is a significant improvement in the TT error in going from 1 to 2 TT NGS WFS, which is due to the tilt estimate in different directions helping to estimate the combinations of quadratic "null modes" that introduce tilt anisoplanatism. There is further improvement in increasing the number of TT NGS WFS, but there is definitely diminishing returns as

Table 3. Residual TT error for the number and type of NGS WFS.

WFS option	TT error (nm)		
	10th percentile	median	90th percentile
1 TT	87	170	341
2 TT	58	122	261
3 TT	53	111	241
4 TT	50	108	231
5 TT	49	106	231
1 TTFA	86	180	287
1 TTFA + 2 TT	47	102	199

the next best star is less bright or adds little to the geometry of the previous ones.

We also consider measuring the focus and astigmatism modes with the NGS using a 2x2 lenslet array. The measuring of focus helps the estimate of the null modes in a similar manner to having multiple TT NGS WFS. Measuring focus comes at a cost in the noise error term, which is due to the increased spot size and the reduction in the number of photons per subaperture. The TT errors for a single TTFA sensor, and for a TTFA sensor in combination with 2 TT sensors are shown in Table 3. There is little improvement in having a single TTFA sensor over a single TT sensor, the improvement in tilt anisoplanatism is largely canceled out by the degradation in the measurement noise term. A combination of multiple TT stars and a TTFA sensor gives the lowest TT error in all cases.

2.D. LGS asterisms and partial correction for different science cases

In this section we compare the sky coverage of three of the different science cases: best case narrow field, field galaxies and GOODS-N. We compare each of these science cases for three different LGS asterism radii: 7.2, 21.6 and 35.9 arc sec. The different science cases have different higher order wavefront errors, galactic latitudes and science field diameters. For the narrow field case, the higher order error is 86nm, the galactic latitude is 10 deg, and the science field diameter is 0.178 arc min. For the Goods-N science case, the higher order error is 218 nm, the galactic latitude is 45 deg, and the science field diameter is 1.09 arc min. Lastly, for the field galaxies case, the higher order error is

Table 4. Residual TT error for three science cases for different LGS asterism radii.

WFS option	TT error (nm)		
	7.1 arc sec radius	21.6 arc sec radius	35.9 arc sec radius
Goods-N	317	284	277
Narrow Field	116	96	94
Field Galaxies	156	131	127

173nm, the galactic latitude is 30 deg, and the science field diameter is 0.7 arc min. In all cases, we consider a 2 arc min diameter patrol field, J band sensing, and the combination of 2 TT sensors + 1 TTFA sensor.

Table 4 shows that there is significant difference in sky coverage for the different science cases, which arises from the expected level of partial correction obtained from the higher order errors, the abundance of stars at the different galactic latitudes, and the increased tilt anisoplanatism of the larger science fields. Table 4 also shows that the LGS asterism radius can have a large impact on the TT errors. The LGS asterism will need to be optimized to minimize the higher order tomography errors and the TT errors.

3. Conclusions

From this trade study, we can conclude that (1) near IR sensing is preferable to visible for the NGS WFS. In particular, a combination of J+H bands gives the best performance. (2) Multiple TT stars can significantly improve the tilt estimate. A further improvement can also be achieved if one of the NGS WFS also measures focus, which aids in estimating the combinations of quadratic null modes. (3) A 2 arc min diameter patrol field for finding NGS is sufficient, there is little benefit to making the field larger due to the reduced partial correction and tilt anisoplanatism from being so far off-axis. (4) The radius of the LGS asterism affects the partial correction of the NGS and hence the sky coverage. The LGS asterism radius needs to be optimized as a function of a weighted sum of the tomography error over the science field and the residual TT error from the partially corrected NGS.

References

1. "The Next Generation Adaptive Optics System at the W.M. Keck Observatory" (2006).

2. R. M. Clare and B. L. Ellerbroek, "Sky Coverage estimates for adaptive optics systems from computations in Zernike space," J. Opt. Soc. Am. A **23**, 418-426 (2006).
3. R. M. Clare, B. L. Ellerbroek, G. Herriot, and J. P. Véran, "Adaptive optics sky coverage modeling for extremely large telescopes," Applied Optics **45**, 8964-8978 (2006).
4. A. Spagna, "Guide star requirements for NGST: deep NIR starcounts and guide star catalogs," STScI-NGST-R-OO13B (2001).
5. J. N. Bahcall and R. M. Soneira, "The universe at faint magnitudes. I. Models for the galaxy and the predicted star counts," Astrophys. J. Supplement **44**, 73-110 (1980).
6. C. Neyman, "Atmospheric Parameters for Mauna Kea," KAON 303 (2004).
7. R. Flicker, "NGAO trade study report: LGS asterism geometry and size," KAON 429 (2006).
8. M. S. Bessell and J. M. Brett, "JHKLM photometry: standard systems, passbands, and intrinsic colors," Pub. Astron. Soc. Pac. **100** 1134-1151 (1988).

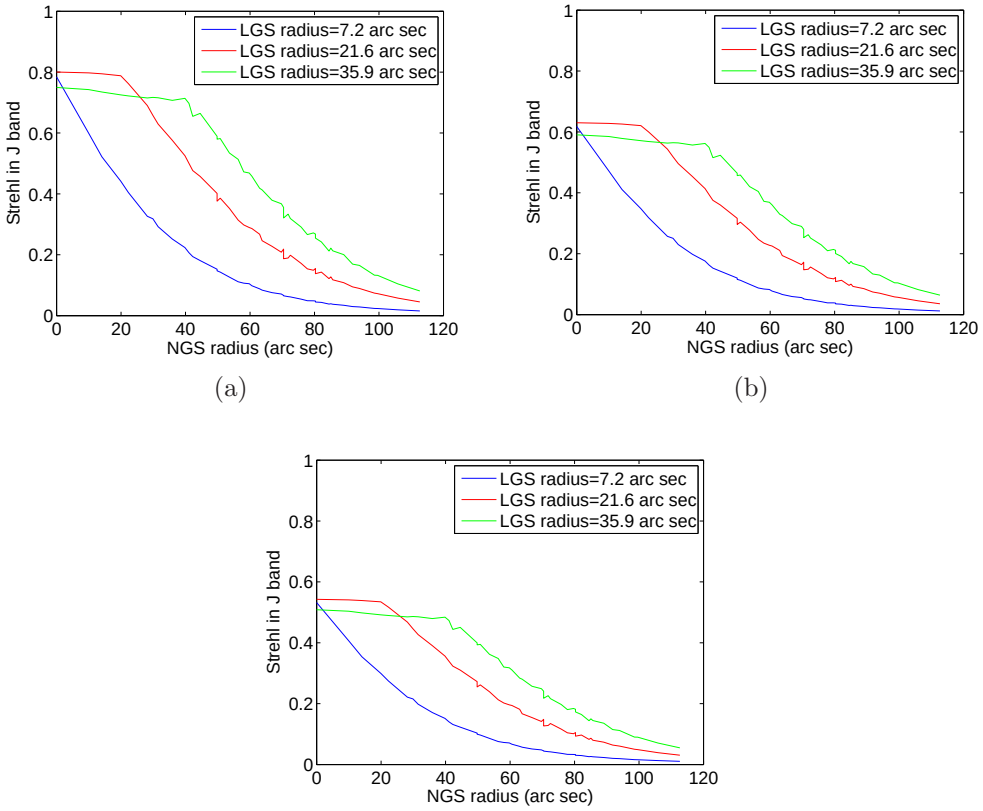

(a) (b)

(c)

Fig. 2. The expected partial correction over the field in J band for a LGS asterism radius of 7.2 arc sec (blue), 21.6 arc sec (red), and 35.9 arc sec (green) for (a) the narrow field science case, (b) the field galaxies science case, and (c) the GOODS-N science case.

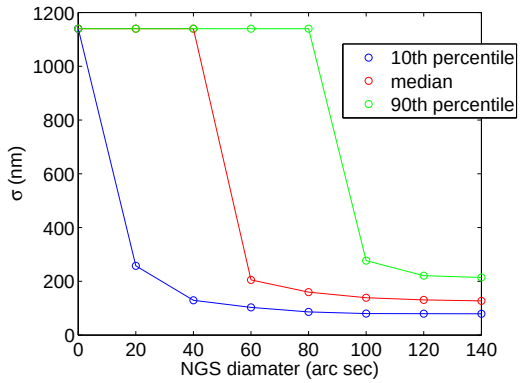

Fig. 3. The median, 10th and 90th percentile TT errors (nm) over 500 NGS constellations versus the patrol field diameter for J band sensing, the field galaxies science case and a 21.6 arc sec LGS asterism radius.